PROPAGATION OF TAU PATHOLOGY IN A MODEL OF EARLY ALZHEIMER'S DISEASE

***Manuela Polydoro*[1*], Alix de Calignon[1], Marc Suárez-Calvet[1,2], Christopher William[1], David H. Adamowicz[1], Kathy J. Kopeikina[1,3], Rose Pitstick[4], Naruhiko Sahara[5], Karen H. Ashe[6], George A. Carlson[4], Tara L. Spires-Jones[1], Bradley T. Hyman[1]**

[1]MassGeneral Inst. for Neurodegenerative Dis. (MIND), MGH/Harvard Med. Sch., Charlestown, MA; [2]Dept. of Neurology, Hosp. de la Santa Creu i Sant Pau, Univ. Autònoma de Barcelona., Barcelona, Spain; [3]Dept. of Anat . and Neurobio., Boston Univ. Sch. of Med., Boston, MA; [4]McLaughlin Res. Inst., Great Falls, MT; [5]Dept of Neuroscience, University of Florida, Gainsville, FL, USA; [6]Dept. of Neurol., Univ. of Minnesota Med. Sch., Minneapolis, MN

***mpolydoro@partners.org**

Abstract

The tauopathies, which include Alzheimer's disease and numerous degenerative disorders, are characterized by deposits of abnormally phosphorylated and misfolded protein tau called neurofibrillary tangles (NFT). In Alzheimer's disease patients, tau pathology appears first in layer II of the entorhinal cortex (EC) and then spreads to the hippocampus and specific cortical areas. The basis of this pattern of stepwise hierarchical vulnerability is unknown. Three possibilities have been suggested: (1) there could be intrinsic differences in regional vulnerability to pathology; (2) pathological changes could potentially spread via trans-synaptic propagation of misfolded proteins or (3) deafferentation or disruption of neural system function could lead to progressive degeneration. We describe a transgenic mouse model in which expression of human tau P301L is restricted to only a subset of the stellate neurons in layer II of entorhinal cortex (EC-II). Human tau proteins were transported to the axon terminals, in the projection zone, where they accumulate from a very early age. Tau pathology progresses from EC transgene-expressing neurons to neurons without detectable transgene expression, first to EC neighboring cells, followed by propagation to neurons downstream in the synaptic circuit such as the dentate gyrus, CA fields of the hippocampus, and cingulate cortex. Human tau protein spreads to these regions and co-aggregates with endogenous mouse tau. With age, synaptic degeneration occurs in the entorhinal target zone and EC neurons are lost. These data suggest that a temporal sequence of progressive misfolding of tau proteins, circuit-based transfer to new cell populations, and deafferentation induced degeneration are part of a single process of tau-induced neurodegeneration.

Conclusions

Taken together, these data indicate that in rTgTauEC mice, tau was transferred to neighboring cells, and to synaptically-connected neurons, suggesting that tau may be released at the synapse. These data suggest that human tau enters adjacent cells that do not have detectable levels of human tau transgene and transmits a misfolded state which recruits endogenous mouse tau into the somatodendritic compartment, contributing to tau aggregation. Our data support the idea that tau induces synaptic destruction when it accumulates in the terminal zones. We cannot distinguish between the possibilities that tau induces dying back terminal degeneration, or that release of tau is synaptotoxic.

Fig. 1

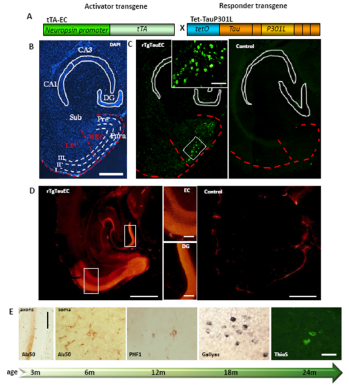

Figure 1. Medial entorhinal cortex-restricted expression of human P301L mutated tau causes progressive tauopathy in EC neurons. (A) The rTgTauEC transgenic mice express human tauP301L under a tetracycline responsive promoter (tetO) and the tetracycline transactivator (tTA) under the neuropsin promoter. (B) Medial horizontal section of rTgTauEC mouse brain stained with DAPI. (C) Fluorescent *in situ* hybridization (FISH) showing human tau mRNA. Scale bars: 1mm and 100mm. (D) Immunohistolabeling with human tau antibody 5A6 (3 months-old age-matched transgenic and control). Scale bars: 1mm and 200mm. (E) Human tau expressing neurons in the MEC develop progressive tau pathology. Scale bar 200 mm and 50 mm.

Fig. 2

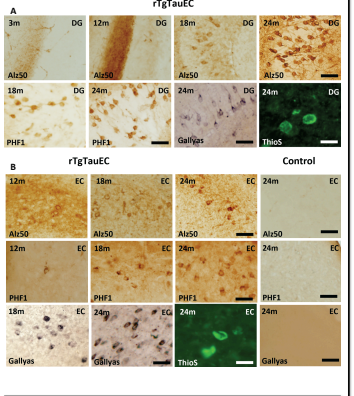

Figure 2. Progression of tau pathology in rTgTauEC EC-II and DG neurons. Immunohistolabeling in MEC of 3 to 24 month-old rTgTauEC and 24 month-old control mice in the DG (A) and EC-II (B). Pathological changes were first observed in the neuronal processes and terminals of the EC-II (A), and later observed in the cell bodies of the EC-II (B). rTgTauEC and brain sections stained with Gallyas silver impregnation, and Thioflavin S showed that late stage neurofibrillary tangles appear in the EC respectively at 18 and 24 months of age. Pathology in the cell bodies of the DG lags behind that in the EC by several months. Scale bar 50 mm for all panels but ThioS which is 10 mm.

Fig. 3

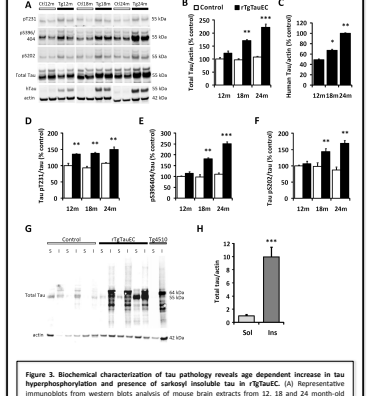

Figure 3. Biochemical characterization of tau pathology reveals age dependent increase in tau hyperphosphorylation and presence of sarkosyl insoluble tau in rTgTauEC. (A) Representative immunoblots from western blots analysis of mouse brain extracts from 12, 18 and 24 month-old rTgTauEC and control mice. Antibodies specific to phospho tau [AT180 (pT231), PHF1 (pS396/404) and CP13 (pS202)], total tau, and human tau (htau) were used. Quantification of immunoblots shows that rTgTauEC mice present an age-dependent increase in total tau (B), human tau (C), and phospho epitopes (D-F) (n=4 mice per group). Sarkosyl-insoluble fractions of tau from whole brain of 24 month-old rTgTauEC, control and 18 month-old rTg4510 mice (positive control). Sarkosyl soluble (S) and insoluble fractions (I) were immunoblotted with total tau antibody (phosphorylation independent, Dako). Representative western blots of sarkosyl fractions are shown. (G). (H) Shows quantification of samples of sarkosyl fractions (n=3 mice per group). Results are expressed as mean ± s.e.m. *P<0.05; **P<0.01; ***P<0.001.

Fig. 4

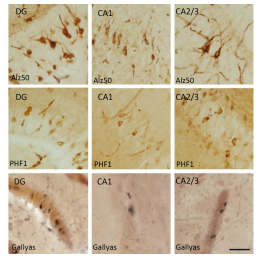

Figure 4. Tau propagates through neural circuits. Several markers of pathological tau accumulation: Alz50 (A), PHF1 (B), and Gallyas silver staining (C), appear in brain regions synaptically connected to EC via the perforant pathway. Scale bar 50 mm.

	3 months	6 months	12 months	18 months	21 months	24 months
MEC axon terminals	Alz50+	Alz50+	Alz50+	Alz50+	Alz50+ clumps	Alz50+ clumps PHF1+ threads Gallyas+ threads
MEC soma	no pathology	Alz50+	Alz50+ PHF1+	Alz50+ PHF1+ Gallyas+	Alz50+ PHF1+ Gallyas+	Alz50+ PHF1+ Gallyas+ ThioS+
DG soma	no pathology	no pathology	no pathology	Alz50+ PHF1+	Alz50+ PHF1+ Gallyas+	Alz50+ PHF1+ Gallyas+ ThioS+
CA2/3 soma	no pathology	no pathology	no pathology	no pathology	Alz50+ PHF1+ Gallyas+	Alz50+ PHF1+ Gallyas+ ThioS+
CA1 soma	no pathology	no pathology	no pathology	no pathology	Alz50+ PHF1+ Gallyas+	Alz50+ PHF1+ Gallyas+

Table: Progression of tau pathology through the EC-hippocampal neural circuit with age in rTgTauEC mice

Fig. 5

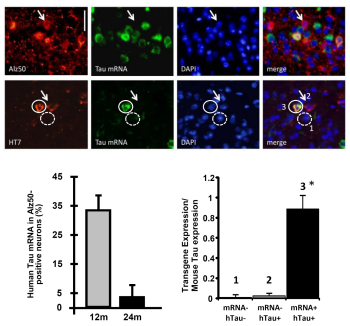

Figure 5. Tau propagates through neural circuits to mRNA-negative cells. FISH for tau mRNA (green), coupled with immunolabeling (red) with Alz50 or HT7 (E) shows absence of mRNA in some cells containing the tau protein (arrows). Scale bar, 20 µm. Stereological quantification of human tau mRNA neurons which are also Alz50 positive in the EC. FISH for MAPT mRNA (green), coupled with immunolabeling using HT7 (red) in the same EC sections from 17 month-old animals was used to laser capture three different population of cells: 1) tau mRNA negative and human protein negative neurons; 2) mRNA negative and human tau protein positive neurons; 3) transgene mRNA positive and human tau protein positive neurons. Total RNA was extracted and qPCR analysis of the cDNA product was carried out using primers against the transgenic human tau construct showing that the neurons which were human tau protein positive and were RNA negative by FISH did not express the tau transgene, confirming tau transmission to neurons that do not express the human tau transgene. Results are expressed as mean ± s.e.m. *P<0.001.

Fig. 6

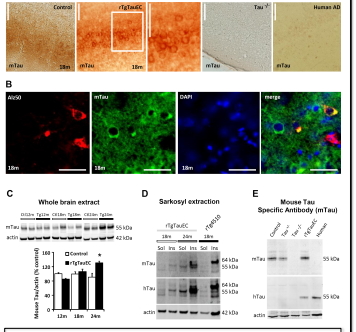

Figure 6. Human tau protein seeds endogenous mouse tau pathology. Immunohistochemistry using a mouse specific tau antibody (mTau) shows normal axonal distribution of mouse tau in the control mice and somatodendritic accumulation of mouse tau in rTgTauEC mice in the EC at 18 months of age (A). The mTau antibody showed no staining in tau knockout mice or human AD brain. Scale bars, 100 µm. Double labeling using Alz50 and mouse tau antibodies shows that Alz50 and mouse tau staining co-localize in neuronal cell bodies (B, Scale bar, 20 µm). (C) Whole brain extracts from rTgTauEC mice at different ages show an age-dependent increase in mouse tau. Representative blots are shown on top and quantification on the bottom (n=4 mice per group). (D) Sarkosyl insoluble and soluble fractions from whole brain of 18 and 24 month-old rTgTauEC probed using the mouse tau specific antibody mTau revealed that sarkosyl insoluble and soluble fractions both contain endogenous mouse tau (E). Immunoblotting of brain extracts using the mouse tau specific antibody confirmed its specificity since it does not recognize protein in tau knockout brain or human AD brain. Results are expressed as mean ± s.e.m. *P<0.05.

Fig. 7

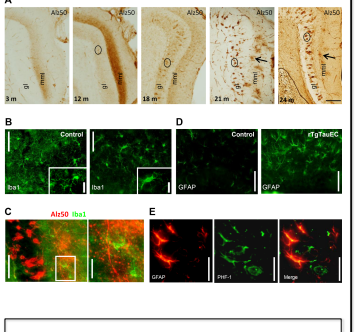

Figure 7. Axon terminals degenerate progressively in the terminal zone of EC-II axons. The terminal zone of axonal projections from the layer II MEC neurons with the granular layer (gl) and the middle-molecular layers (mml) which express the human tau transgene developed early accumulation of misfolded tau (Alz50 staining, A) which intensified up to 12 months of age. At 18 months, the terminal staining with Alz50 became fainter with DG neurons in the granular cell layer becoming more prominently stained. At 21 and 24 months, Alz50 staining in the terminal zone was patchy indicating degeneration of Alz50 containing axons (Scale bar 100 mm, A). Concomitant with this axonal degeneration, we observe increased microglial activation (Iba1 staining) at 24 months of age in rTgTauEC mice in the molecular layer of the dentate gyrus (B) Double Immunohistolabeling with Alz50 and Iba1 shows that the patches of Alz50 staining of the axon terminals in the middle molecular layer of dentate gyrus are surrounded by activated microglia (C, shown in higher magnification in the inset. Scale bars, 50 mm left panel), and 20 mm right panel). GFAP labeled astrocytes are more prevalent in rTgTauEC brain than controls (D. Scale bar, 50 mm). Co-localization of GFAP and PHF1-positive aggregates indicate uptake of tau by astrocytes (E, Scale bar, 20 mm).

Fig. 8

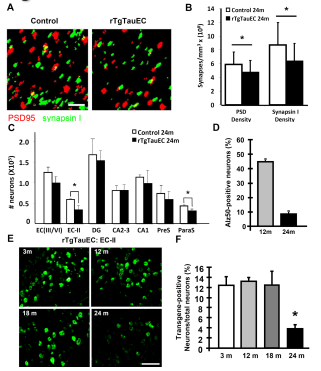

Figure 8: Synaptic loss in the target zone of the perforant pathway and loss of EC-II neurons in rTgTauEC mice. (A and B) Array tomography labeling of pre and postsynaptic structures in the middle molecular layer of the DG. scale bar 2 mm. (C) Neuronal counts in different brain regions (EC 3-6, layers III to VI of entorhinal cortex; EC 2, layer II; DG, granular layer of dentate gyrus; CA2-3; CA1; presubiculum; parasubiculum). (D) Stereological quantification of Alz50 positive neurons in the EC. (E and F) Levels of transgene expression: loss of neurons could not be explained by an increase in transgene expression assessed by stereological counts of tau mRNA positive neurons in the MEC. Scale bar 100mm. Results are expressed as mean ± s.e.m. *P<0.05.

Supported by an Alzheimer's Association Zenith award; NIH grants AG08487, AG026249, K08NS069811, K99AG33670, R21AG038835-01A1, and R21 NS067127; American Health Assistance Foundation (AHAF) Grant A2011086